Theoretical and Experimental Investigation about the Influence of Peltier Effect on the Temperature Loss and Performance Loss of Thermoelectric Generator

Li, Xingjun; Wang, Jun; Meng, Qingtian; Yu, Dan

Published in:
Energy Technology

DOI (link to publication from Publisher):
10.1002/ente.202100895

Publication date:
2022

Document Version
Accepted author manuscript, peer reviewed version

Application solutions for lithium-ion secondary battery analysis

Lithium-ion secondary batteries with high-energy density are emerging as a new energy source. Materials for analyzing battery contents such as positive electrode materials, negative electrode materials, separators, and electrolytes are vital in research development and quality control.

To improve battery characteristics and safety, it's essential to understand the internal state of the battery through multiple analyses. Explore our application solutions for lithium-ion secondary battery analysis that combine analytical instruments such as FT-IR, ICP-OES, GC/MS, and DSC.

Learn more at
www.perkinelmer.com/battery

PerkinElmer®
For the Better

Theoretical and experimental investigation about the influence of Peltier effect on the temperature loss and performance loss of thermoelectric generator

Xingjun Li[1,2], Jun Wang[1,], Qingtian Meng[1], Dan Yu[1]*

[1] X. Li, J. Wang, Q. Meng and D. Yu

School of Automotive and Traffic Engineering, Jiangsu University, Zhenjiang 212013, China

E-mail: qcwjun@ujs.edu.cn

[2] X. Li

Department of Energy, Aalborg University, Pontoppidanstraede 111,9220 Aalborg East, Denmark

Email: xinli@energy.aau.dk

Abstract:

Thermoelectric generator (TEG) has a great potential in low grade waste heat recovery and there are some researches about the influence of Peltier effect on it. However, most of them only consider the total performance changes, such as the variation of power and efficiency, due to the Peltier effect and ignore the impact of Peltier effect on the temperature of TEG, which is the core reason of the performance changes. In order to investigate how the Peltier effect affects the temperature loss at the two both sides of TEG respectively and performance, an experimental setup was built and an analytical model was derived. The result shows that the temperature loss at the cold side is less than that of the hot side. The power loss has the liner relation with the product of the temperature difference and temperature loss. And the maximum loss of power, energy efficiency and exergy efficiency occurs at a particular load range. Within that range, power, energy efficiency and exergy efficiency reach the maximum respectively. According to the results, the suggestion of thermal resistance optimization for TEG is provided.

Keywords:

thermoelectric generator, peltier effect, temperature loss, exergy efficiency

This article has been accepted for publication and undergone full peer review but has not been through the copyediting, typesetting, pagination and proofreading process, which may lead to differences between this version and the Version of Record. Please cite this article as doi: 10.1002/ente.202100895.

1. Introduction

Thermoelectric generator (TEG) is a power generation device that can utilize the low grade heat when it is subjected to the temperature difference. Different from other waste heat recovery devices, TEG has numerous advantages like no moving parts, silent operation and high reliability[1-4]. It has a wide range of applications, including the combined heat and power system for stoves[5-7], body heat harvesting[8], automobile[9-12] and aircraft and helicopters[13]. However, its power and conversion efficiency are extremely low, especially in lower temperature difference[14].

The reduction of effective temperature difference for TEG is caused by a number of factors, one of them is thermal resistance layers of passive components like ceramic substrates. In the work of A. Ferrario[15], a temperature iterative model considering the thermal loss in passive layer was built for the calculation of the junction temperature, and it is found that the temperature loss increases with the increase of the hot side temperature. Li, Zheng et al.[16] put forward a simplified temperature distribution model for stove-powered TEG and the result shows that the effective temperature difference is lower than the imposed temperature difference due to the existence of thermal grease and ceramic substrate. However, only one load resistance was considered. Wang, Xie et al.[17] quantified the influence of thermal contact resistance on the performance of TEG. In their research, the reduction of the thermal contact resistance was caused by the application of the interface material and the increase of loading pressures. The result showed that the performance is enhanced by reducing the thermal contact resistance. Karthick, Suresh et al.[18] evaluated further many factors affecting the thermal contact resistance and the result showed that the thermal conductivity for interface material has an optimal value and the contact pressure and surface roughness have non-obvious effect when the optimal thermal conductivity is adopted. Zhang, Wang et al.[19] studied the impact of the external and internal interface layers on the performance of annular thermoelectric generators and it is also found that there is obvious reduction for the performance when interface layers were taken into consideration. In the above literatures, however, the reduction of effective temperature difference is caused by the thermal resistance layers and Peltier effect at the same time, and the effect of the Peltier effect has not been ruled out.

What's more, although cooling mode for thermoelectric module is based on the Peltier effect, but it has side effect for power generation mode[9]. Liao et al.[20] investigated the influence of Peltier effect on performance of TEG through the numerical model, the result shows the reduction of

effective temperature difference and the inconsistency between the load resistance and internal resistance when the power is maximum. Besides, the Peltier effect is more significant when the heat transfer boundary is weak. However, the hot and cold side temperature of TEG was regarded as the constant in the study, which is hard happen in real life. Further, Wang and Cao et al.[21] researched how Peltier effect affects the output performance and the deviation of maximum power point by experiment. It is found that the actual power is less than the theoretical result and the maximum power point deviates from the theoretical point. In short, all of these involve the variation of the cold side temperature to the hot side temperature[22].

Previous studies about the influence of Peltier effect on performance of TEG mainly focus on the hot and cold side surfaces of the TEG and it is always studied mixed with the thermal resistance layer also causing temperature loss. However, the Peltier effect happens at the junction of p-type and n-type junctions. The influence of Peltier effect at the hot and cold side on the performance was not studied respectively. Besides, the side temperature of TEG is always regarded as a constant in prior studies. The relationship between the power loss and temperature loss is also not studied. In this paper, therefore, the influence of Peltier effect at two sides on the temperature loss and performance loss is comparatively studied when the influence of thermal resistance layer is eliminated. And the side temperature is obtained through the experiment rather than a constant. The thermoelectric performance loss is evaluated by analytical model. The result thoroughly explains the difference of temperature loss at two sides of TEG and it is more effective to reduce the thermal resistance of hot side for higher temperature difference. In addition, the exergy efficiency is discussed because it is effective to identify actual irreversibilities of TEG[23-28].

2. Theoretical model

A commercial TEG contains many identical thermoelectric (TE) couples to augment its electrical potential, which are connected electrically in series and thermally in parallel. A single TE couple comprises p-type and n-type semiconductor, copper strips and ceramic substrates, as shown in **Figure 1**.

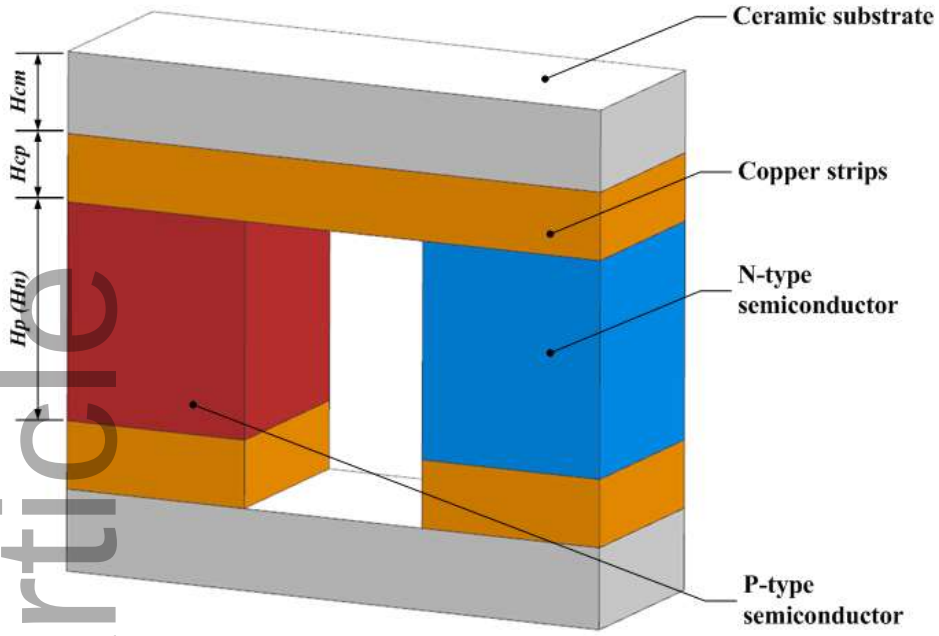

Figure 1 Diagram of a single TE couple

For a TE couple, its energy conversion process involves Seebeck effect, Peltier effect, Fourier effect, Thomson effect and Joule effect. In order to simplify analysis, some assumptions are considered as follows:

(1) Joule heat is neglected based the low temperature gradient approximation mentioned in the research of S. Vostrikov[29] and Thomson heat is also neglected, because their magnitudes occupy a small portion of the total heat flux for Bi_2Te_3. This assumption is vital. Based on this assumption, the temperature distribution could be regarded as linear distribution.

(2) Heat transfer between the sides of one TE couple and another TE couple and the environment is disregarded, because the outside of TEG in the experiment will be filled with the thermal insulation material.

(3) TE materials have variable properties while others have constant properties.

Therefore, the schematic of energy stream of TEG at open-circuit state and closed-circuit state is depicted in **Figure 2**. When the TEG is at open-circuit state, the input heat flow $Q_{\square}$ from hot side is equal to the output heat flow Q_c, which is the sum of conductive heat about p-type and n-type semiconductor (i.e., $Q_{c\square,p}$ and $Q_{c\square,n}$). When the current flows through the TE couple, Peltier heat at all junctions (i.e., $Q_{p\square,n\square}$, $Q_{p\square,nc}$, $Q_{p\square,p\square}$, $Q_{p\square,pc}$) will appear with conductive heat simultaneously.

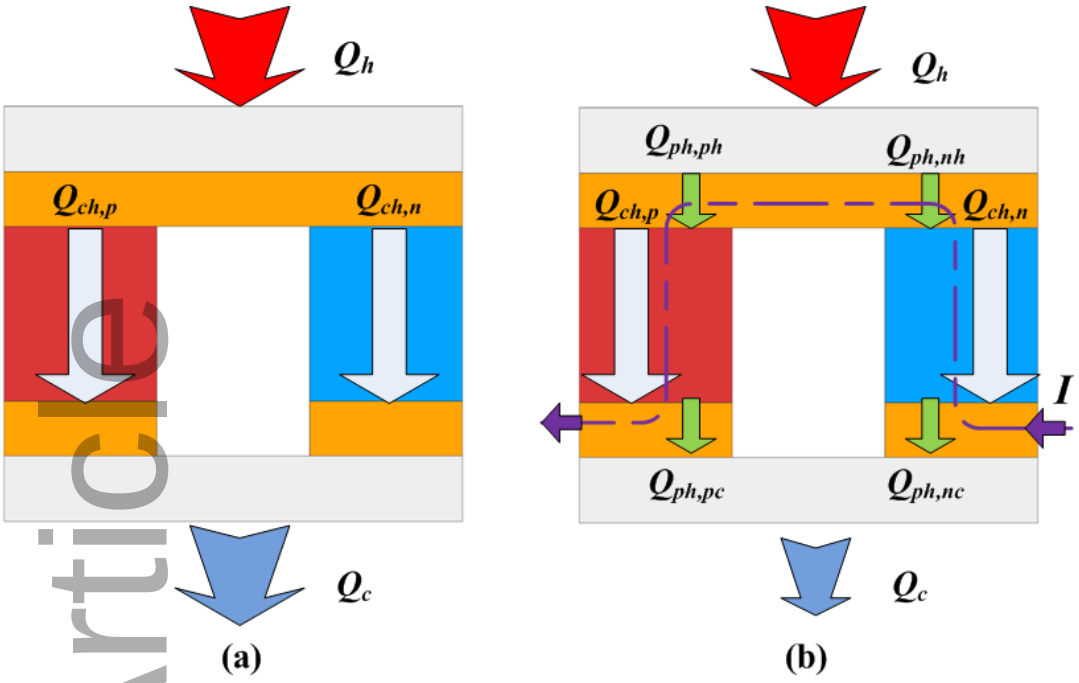

Figure 2 Energy stream of TEG (a) open-circuit state; (b) closed-circuit state

The schematic of thermal resistance for TEG is shown in **Figure 3**, the temperature of TEG can be calculated as follows[16, 30] :

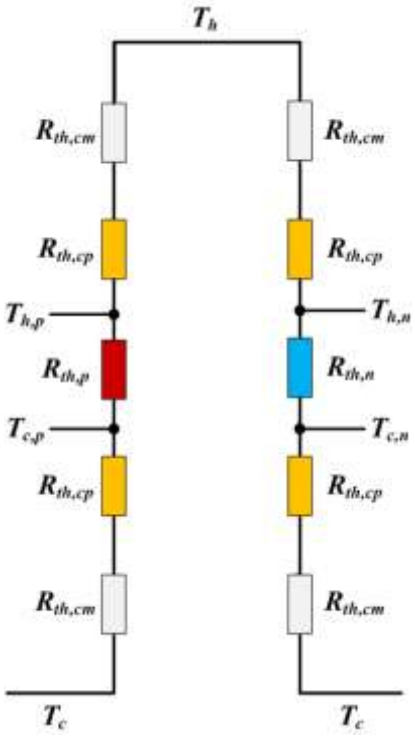

Figure 3 The schematic of thermal resistance

$$T_{□,p} = \frac{R_{t□,p}+R_{t□,cm}+R_{t□,cp}}{R_{t□,p}+2\left(R_{t□,cm}+R_{t□,cp}\right)}\left(T_{□}-T_c\right)+T_c \quad (1)$$

$$T_{c,p} = \frac{R_{t□,cm}+R_{t□,cp}}{R_{t□,p}+2\left(R_{t□,cm}+R_{t□,cp}\right)}\left(T_{□}-T_c\right)+T_c \quad (2)$$

$$T_{□,n} = \frac{R_{t□,n}+R_{t□,cm}+R_{t□,cp}}{R_{t□,n}+2\left(R_{t□,cm}+R_{t□,cp}\right)}(T_{□} - T_c) + T_c \quad (3)$$

$$T_{c,n} = \frac{R_{t□,cm}+R_{t□,cp}}{R_{t□,n}+2\left(R_{t□,cm}+R_{t□,cp}\right)}(T_{□} - T_c) + T_c \quad (4)$$

Where $R_{t□,cm}$ and $R_{t□,cp}$ are the thermal resistance of ceramic substrate and copper strips separately and could be obtained as follows:

$$R_{t□,cm} = \frac{H_{cm}}{\lambda_{cm}A_{cm}} \quad (5)$$

$$R_{t□,cp} = \frac{H_{cp}}{\lambda_{cp}A_{cp}} \quad (6)$$

For the calculation of thermal resistance of P-type and N-type semiconductor, $R_{t□,p}$ and $R_{t□,n}$, is different from above calculations and are given as follows:

$$R_{t□,p} = \frac{H_p}{\lambda_{m,p}A_p} \quad (7)$$

$$R_{t□,n} = \frac{H_n}{\lambda_{m,n}A_n} \quad (8)$$

Where $\lambda_{m,p}$ and $\lambda_{m,n}$ is the thermal conductivity of P-type and N-type semiconductor under the average temperature T_m as follows:

$$T_m = \frac{(T_{□}+T_c)}{2} \quad (9)$$

$$\lambda_{m,p} = \lambda_p(T_m),\ \lambda_{m,n} = \lambda_n(T_m) \quad (10)$$

Furthermore, an open-circuit voltage will be generated, as shown in **Equation 11**:

$$U_{oc} = n(\int_{T_{c,p}}^{T_{□,p}} \alpha_p\, dT) - n(\int_{T_{c,n}}^{T_{□,n}} \alpha_n dT) \quad (11)$$

The output performance of TEG will be derived as following equations:

$$U_o = IR_L = \frac{U_{oc}R_L}{R_{teg}+R_L} \quad (12)$$

Where R_{teg} is internal resistance and could be calculated as follows:

$$R_{teg} = R_p + R_n + R_{cp} = n\left(\int_{T_{c,p}}^{T_{□,p}} \rho_p dT\right)\frac{H_P}{\Delta T_p A_p} + n\left(\int_{T_{c,n}}^{T_{□,n}} \rho_n dT\right)\frac{H_n}{\Delta T_n A_n} + 2n\frac{\rho_{cp}H_{cp}}{A_{cp}} \quad (13)$$

$$P_{out} = (\frac{U_{oc}}{R_{teg}+R_L})^2 R_L \quad (14)$$

$$Q_{c□} = Q_{c□,p} + Q_{c□,n} = n(\frac{A_p}{l_p}\int_{T_{c,p}}^{T_{□,p}} \lambda_p dT + \frac{A_n}{l_n}\int_{T_{c,n}}^{T_{□,n}} \lambda_n dT) \quad (15)$$

$$Q_{p□,□} = Q_{p□,p□} + Q_{p□,n□} = n\alpha_p\left(T_{□,p}\right)IT_{□,p} - n\alpha_n\left(T_{□,n}\right)IT_{□,n} \quad (16)$$

$$Q_{□} = Q_{c□} + Q_{p□,□} \quad (17)$$

$$\eta = \frac{P_{out}}{Q_{□}} \quad (18)$$

Considering the first and second law of thermodynamics, the exergy balance of TEG could be given as:

$$Ex_{in} = Ex_{out} + Irreversibilities \quad (19)$$

For TEG, the irreversibilities include internal and external irreversibilities[28]. The internal irreversibilities are caused due to the properties of materials in this study while the external irreversibilities are resulted from irreversible heat transfer. In **Equation 19**, Ex_{in} is the exergy input to TEG and is calculated as follow:

$$Ex_{in} = Q_{□}(1 - \frac{T_o}{T_{□,pn}}) \quad (20)$$

Where the T_o is the ambient temperature and the $T_{□,pn}$ is the average temperature of the hot junction temperature of P-type and N-type semiconductor which is expressed as $T_{□,pn} = \frac{(T_{□,p}+T_{□,n})}{2}$. The output power ($P_{out}$) is regarded as the exergy output Ex_{out}. Finally, the exergy efficiency of the TEG is expressed as:

$$\varepsilon = \frac{P_{out}}{Ex_{in}} \quad (21)$$

3. Experimental setup

In order to further study how the Peltier effect impacts the junction temperature and performance of TEG, a special experiment setup was built as shown in **Figure 4**. The thermal grease layer with suitable thickness and thermal conductivity was used to obstruct the effect of heat/cold source and highlight the Peltier effect simultaneously, and 2mm with 3.5W/mK was founded to be an optimal parameter by preliminary experiment. In this study, the thermal grease layer was filled in two special glass panes, which inner hole size is 50mm(length) × 50mm(width) × 2mm(height). The TEG was placed between the upper and bottom thermal grease. The TEG adopted in this experiment was TEG1-199-1.4-1.6 which is composed of 199 thermocouples and its total geometric parameter is 50mm × 50mm × 3.8mm. The dimension of a single thermoelement is 1.4mm(length) × 1.4mm(width) × 1.6mm(height). And the thicknesses of ceramic substrate and copper strips are 0.6mm and 0.5mm respectively. Physical parameters provided by manufacturer (Fuxin Technology Co., Ltd., China) are listed in **Table 1**. A thermostatic heater (HP-2020) was used as hot source and it can supply stable heat flux. An aluminum water cooled heat sink was connected to water pipe and the water temperature at inlet of the aluminum water block was kept as 12□. The fastening bolt was used to keep same pressure at both sides. The ambient temperature was 12□.

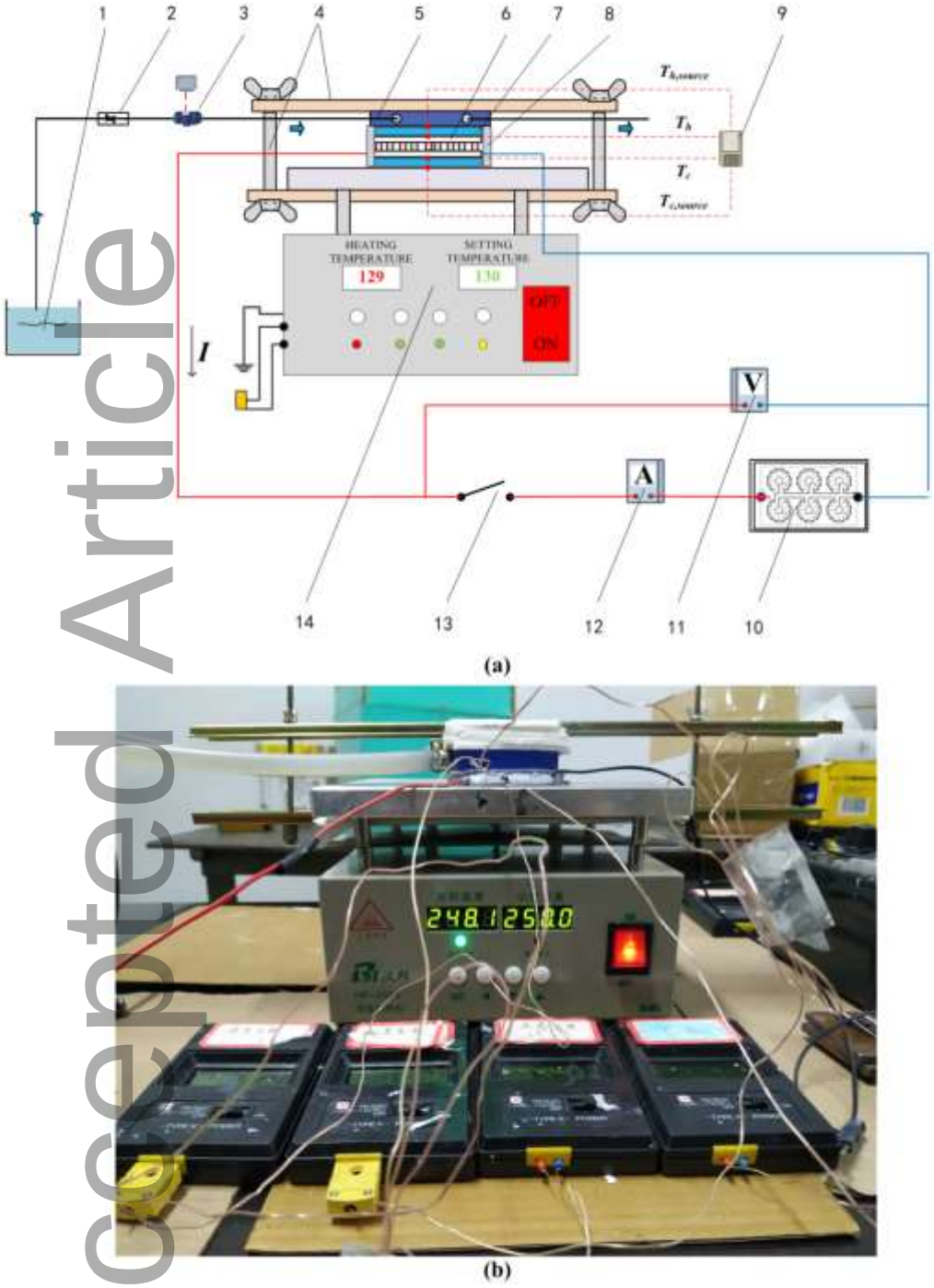

Figure 4 The experimental setup (a)schematic diagram (b) photograph, (1) city water tank; (2) valve; (3) flowmeter; (4) clamping device; (5) aluminum water cooled heat sink; (6) TEG; (7) thermal grease layer; (8) thermal insulation material; (9) K-type thermocouples and digital display; (10) Variable resistance box; (11) Voltmeter; (12) Ammeter; (13) Switch; (14) Thermostatic heater.

Table 1 Physical parameters

Paramet	Seebeck	Thermal	Electrical

ers / Components	conductivity [V/K]	conductivity [$W \cdot m^{-1} \cdot K^{-1}$]	resistivity [$\Omega \cdot m$]
P-type semiconductor	$(-5.94524 \times 10^{-8} \times T^3 + 6.0534 \times 10^{-5} \times T^2 - 1.77636 \times 10^{-2} \times T + 2.93309) \times 10^{-4}$	$-1.3588 \times 10^{-8} \times T^3 + 4.65818 \times 10^{-5} \times T^2 - 0.03246 \times T + 8.05499$	$(8.55608 \times 10^{-8} \times T^3 - 8.9378 \times 10^{-5} \times T^2 + 3.7199 \times 10^{-2} \times T - 4.6148) \times 10^{-5}$
N-type semiconductor	$(3.14252 \times 10^{-8} \times T^3 - 3.07869 \times 10^{-5} \times T^2 + 8.26791 \times 10^{-3} \times T - 2.09365) \times 10^{-4}$	$5.32452 \times 10^{-8} \times T^3 - 3.75249 \times 10^{-5} \times T^2 + 0.0042 \times T + 2.69599$	$(-2.9129 \times 10^{-8} \times T^3 + 3.31546 \times 10^{-5} \times T^2 - 8.59115 \times 10^{-3} \times T + 1.360321) \times 10^{-5}$
Ceramic substrate	-	22	-
Copper strips	-	385	1.75×10^{-8}

During the experiment process, the hot source temperature ($T_{□,source}$), i.e., thermostatic heater surface temperature, was changed according to the setting temperature. The cooling water flow rate was changed by the flow valve and measured by the flowmeter. The hot source temperature ($T_{□,source}$), the hot side temperature of TEG ($T_{□}$), the cold side temperature of TEG (T_c) and the cold source temperature ($T_{c,source}$) were measured by four K-type thermocouples (accuracy, ± 0.1□). Before the formal experiment, the four thermocouples are calibrated to make their results consistent. The output voltage and current could be measured by changing the load resistance and the data could be recorded using the voltmeter and ammeter respectively. Particularly, the open-circuit voltage could be obtained when the switch is at open state. All parameters were recorded after reaching a stable state.

4. Results and discussion

The main innovation point of this study is to compare the influence of the Peltier effect on the both sides temperature of TEG and then thermoelectric performance through the combination of analytic calculation and experiment. At first, the appropriate cold water flow rate for subsequent study was determined. Then, the open-circuit voltage at different hot side temperatures of TEG were measured and compared with theoretical result for verifying the temperature distribution model. After that, relevant numerical analysis was performed by utilizing the temperature of TEG both sides and other data from experiment after connecting load resistance.

4.1 The cold water flow rate

In order to focus on the Peltier effect, other influence factors should be excluded as much as possible. Therefore, the effect of cooling water flow rate on the cold source temperature, cold side temperature and open-circuit voltage at different hot side temperatures (50□, 90□, 130□ and 170□) was studied. As shown in **Figure 5**, the cold source temperature, cold side temperature drop dramatically at first and then keep a slightly downward tendency when the cold water flow rate increases from the 0 L/min to others. This can be attributed to the change in heat transfer mode (i.e., from heat conduction to convective heat transfer with different heat transfer coefficient). Accordingly, the open-circuit voltage has an opposite trend. Furthermore, all the open-circuit voltages start to level off when the cold water flow rate increases from 2.6 L/min to 4.25 L/min. In view of the fluctuation of water flow and energy balance, the appropriate cold water flow rate is set as 3.5L/min for follow-up studies.

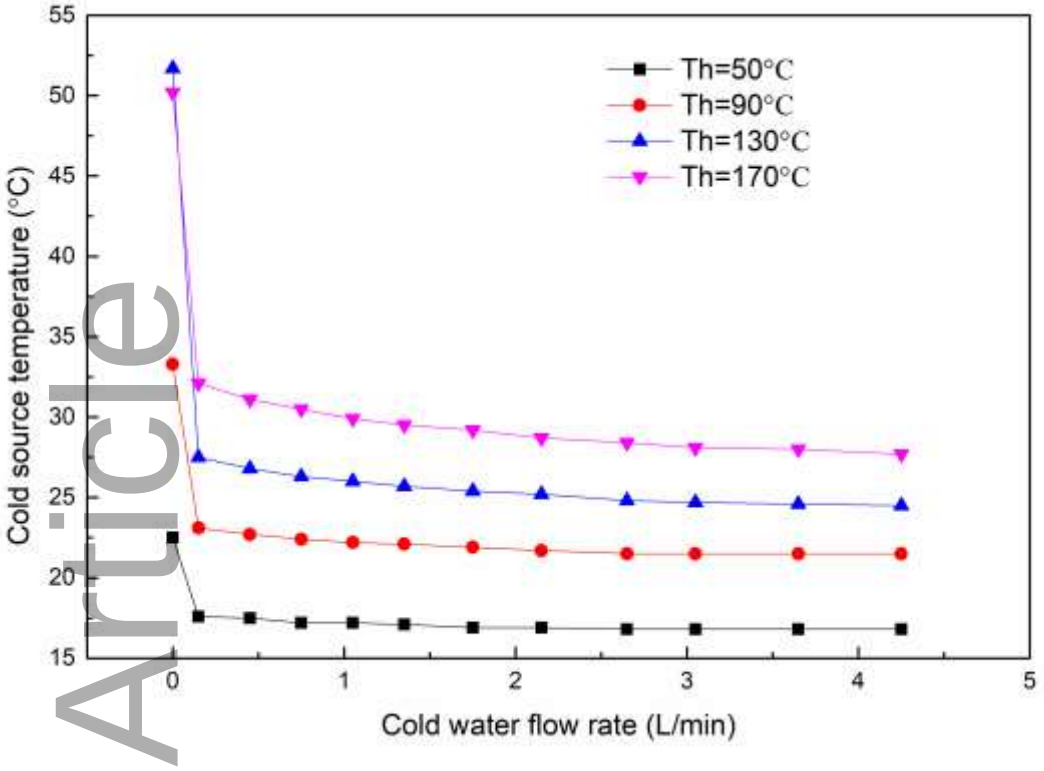

(a)

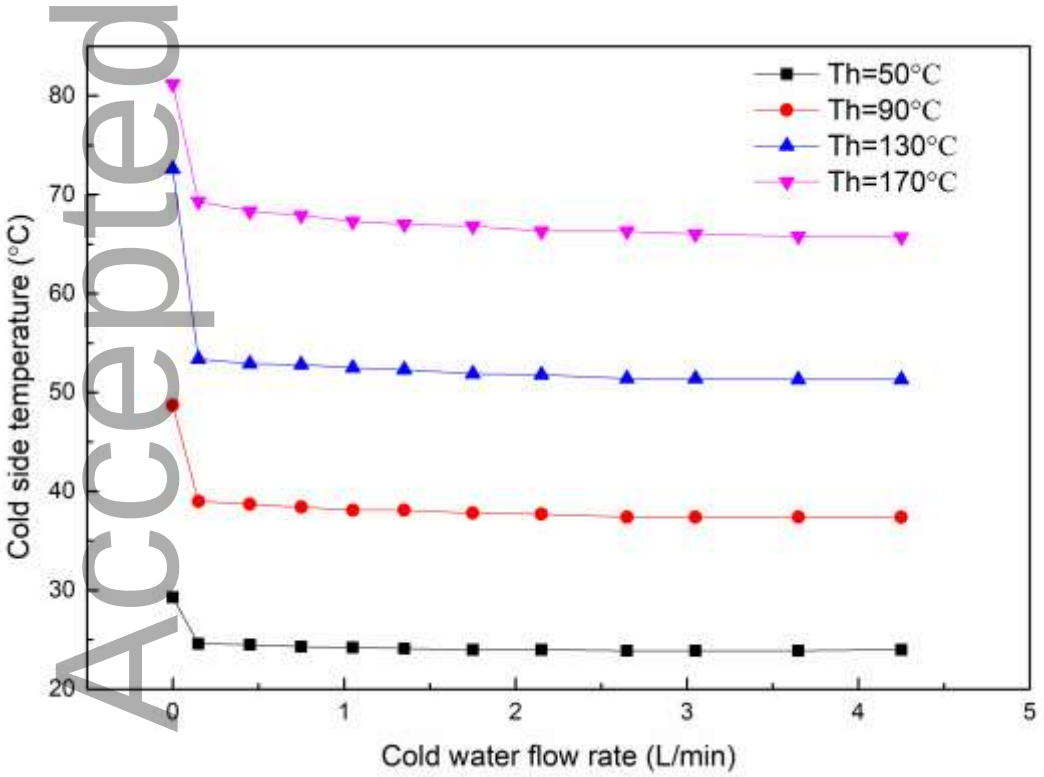

(b)

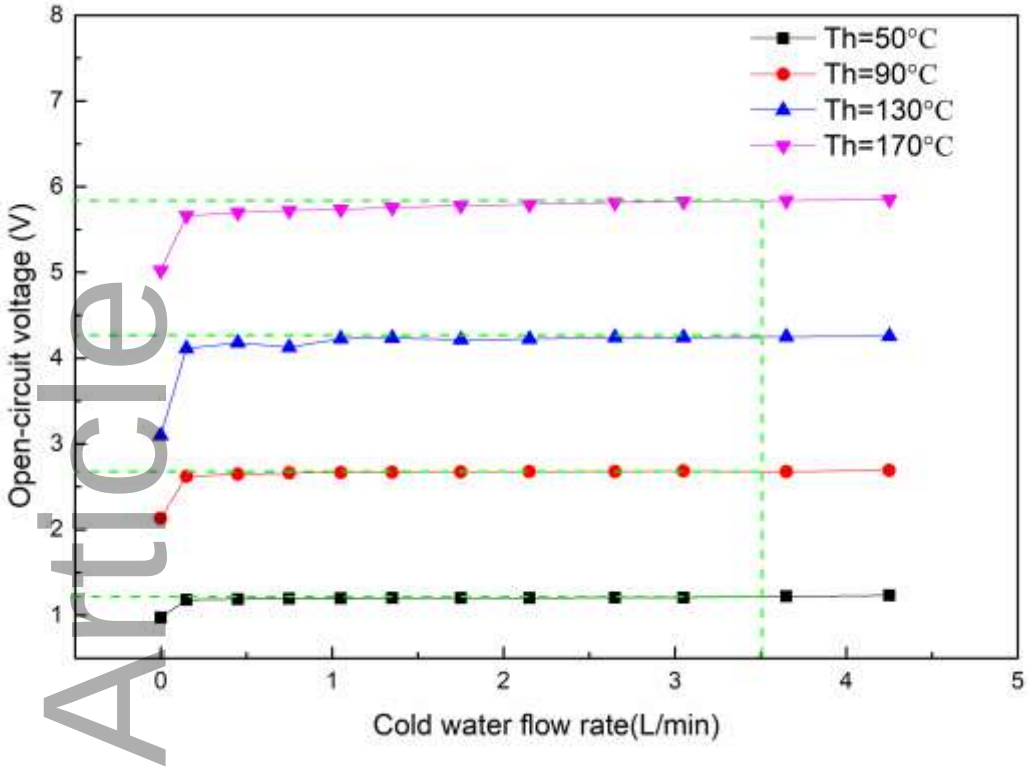

(c)

Figure 5 Cold source temperature (a) Cold side temperature (b) and open-circuit voltage with cold water flow rate.

4.2 Theoretical model verification

In practice, the temperature at the PN junction can't be obtained directly by experiment due to the existence of thermal resistance layers, but open-circuit voltage can be measured conveniently using voltmeter and can be used as a validation parameter. In order to obtain the temperature at the PN junction, this study built a temperature distribution model based on **Equation 1**-**Equation 4** for TE performance evaluation. Then the open-circuit voltage is calculated based on **Equation 1**1 and compared with experiment results as shown in **Figure 6**. From **Figure 6**, it is found that the relative error between the theoretical results and experiment results reaches its maximum at hot side temperature is 50□, with 14%. And it declines with the increase of the hot side temperature. The error may be caused by the thermal loss of conductive and radiative heat transfer in TEG and the neglect of the welding layer. The temperature distribution model shows good agreement with experiment and can be used for subsequent evaluation.

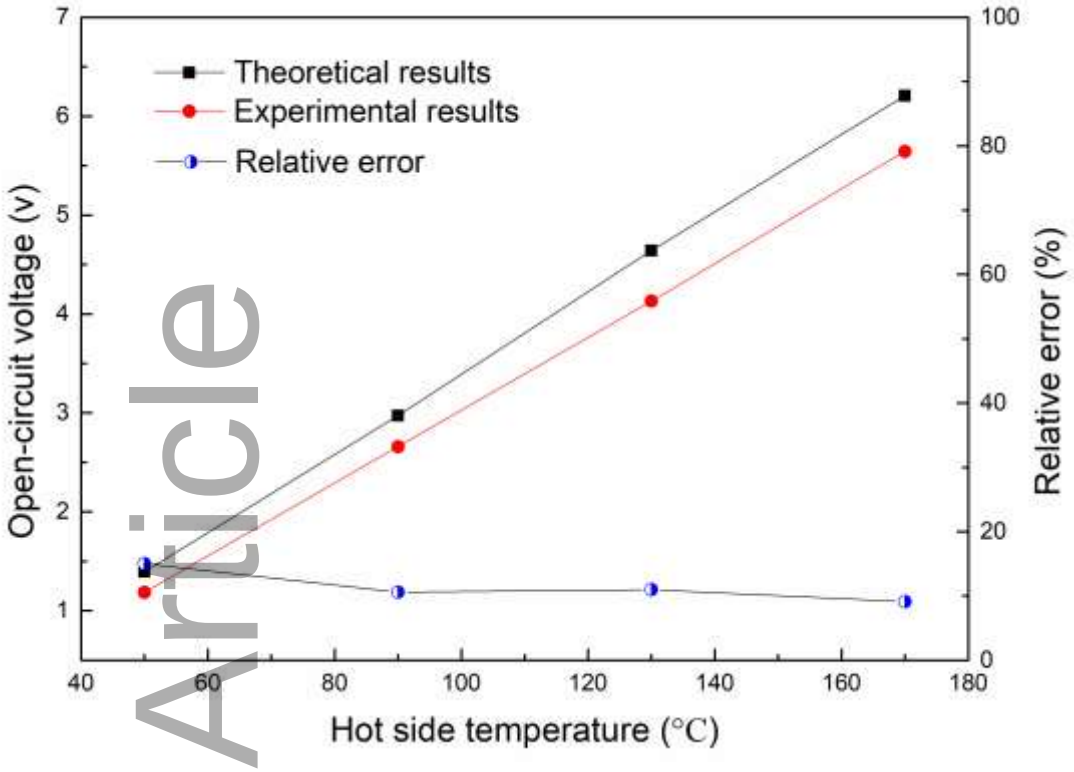

Figure 6 Verification of temperature distribution

4.3 Influence of Peltier effect on the temperature loss

After the model is validated, the side temperature of TEG at different load resistance measured from experiment could be used the calculation of the junction temperatures of P-type and N-type semiconductor based on the **Equation 1**-**Equation 4**, which is the real temperatures for calculation of thermoelectric performance. **Figure 7** exhibits variation trend of the junction temperatures at different hot side temperature. Compared with the junction temperature at open-circuit state, all the hot junction temperature T_{pn} is less than the hot junction temperature at open-circuit state $T_{pn,oc}$ from beginning to end, and it increases with the increase of the load resistance, while the cold junction temperature T_{cpn} shows the opposite trend. It means that the effect temperature difference ΔT increases as the load resistance increases. However, the effect temperature difference ΔT is lower than that in open-circuit state. That can be attributed to the Peltier heat, which has negative effect on the temperature difference. When the load resistance increases, the current also decreases and the Peltier heat at both junctions decreases gradually to the near zero accordingly, which lead to the junction temperature close to that at open-circuit state.

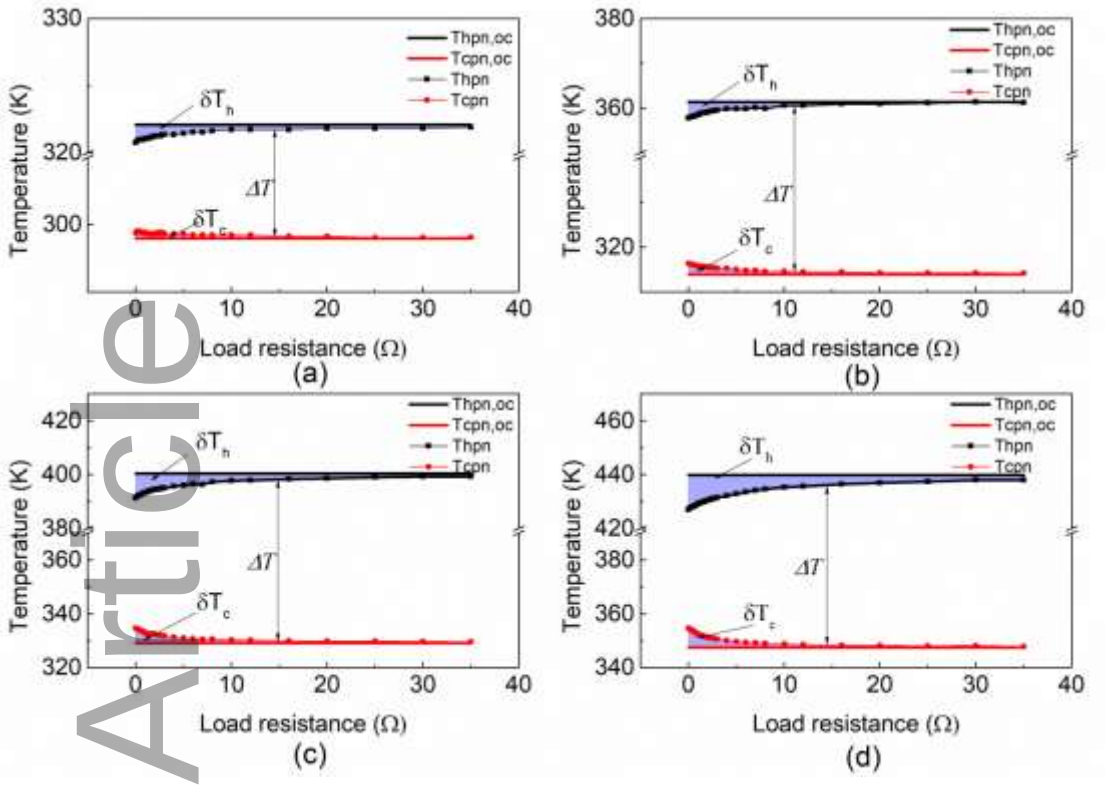

Figure 7 Junction temperature profiles for TEG at different hot side temperature (a) Th = 50□ (b) Th = 90□ (c) Th = 130□ (d) Th = 170□

Further, it is found that the hot junction temperature loss δT_h (i.e., $\delta T_h = T_{hpn,oc} - T_{hpn}$) is greater than the cold conjunction temperature loss δT_c (i.e., $\delta T_c = T_{cpn,oc} - T_{cpn}$) obviously at different hot side temperature as shown in **Figure 8**. And the difference between the two decreases as the load resistance increases.

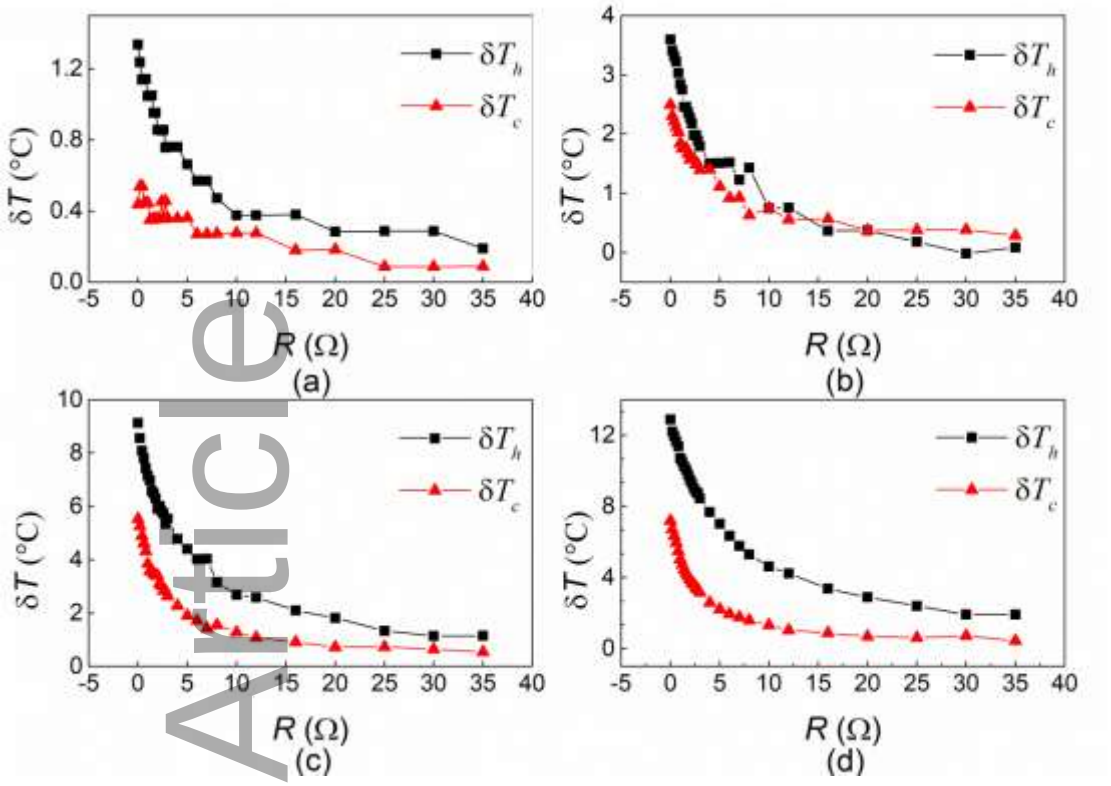

Figure 8 Comparison of temperature loss at hot and cold junction at different hot side temperature of TEG （a） Th = 50℃ (b) Th = 90℃ (c) Th = 130℃ (d) Th = 170℃

In order to fully explain this phenomenon, the source temperature $T_{h,source}$, $T_{c,source}$ measured in experiment versus load resistance was studied first. As shown in **Figure 9**, it could be seen that cold source temperature $T_{c,source}$ changes a little with load resistance, but the hot source temperature $T_{h,source}$ increases with the increase of load resistance. In other words, the source temperatures $T_{h,source}$, $T_{c,source}$ being measured are not the true source temperatures. And modes of heating and cooling in the experiment could be viewed as constant heat flux. There must be two limiting positions that temperatures are unchanged, which are defined as true source temperatures$T^*_{h,source}$, $T^*_{c,source}$. For example, the temperature could be regarded as constant in infinite plate occasions. And obtained experiment result is different from the result in the result of M. Liao[20] where the side temperatures of TEG regard as constant. In fact, the side temperatures of TEG will vary with the load resistance. Then, taking P-type semiconductor as an example, its thermal resistance and energy flow schematic diagram is shown in **Figure 10**. From the **Figure 10**, the variation of heat flows at the hot side and cold side is determined by the Peltier heat and junction temperatures are given at follows:

$$T_{h,p} = T^*_{h,source} - Q_h \cdot R_{th,h} = T^*_{h,source} - (Q_{h,source} + Q_{ph,h}) \cdot R_{th,h} \quad (22)$$

$$T_{c,p} = T^*_{c,source} + Q_c \cdot R_{th,c} = T^*_{c,source} + (Q_{c,source} + Q_{ph,c}) \cdot R_{th,c} \quad (23)$$

In the above equations, $Q_{□,source}$ and $Q_{c,source}$ are constants, the thermal resistances also can

be regarded as constants according to the experiment result. However, the change amplitude of the Peltier heat at the hot junction $Q_{p\square,\square}$ is larger than that at the cold junction $Q_{ph,c}$ at a random circuit due to difference of the junction temperature, so the temperature loss at the hot junction $\delta T_{\square}$ is larger than that at the cold junction δT_c accordingly. In addition, in order to obtain larger temperature difference, smaller thermal resistances between the heat source and junction are necessary because it can offset the influence Peltier heat partly. And changing the thermal resistance at the hot side is more important and effective for a large temperature difference.

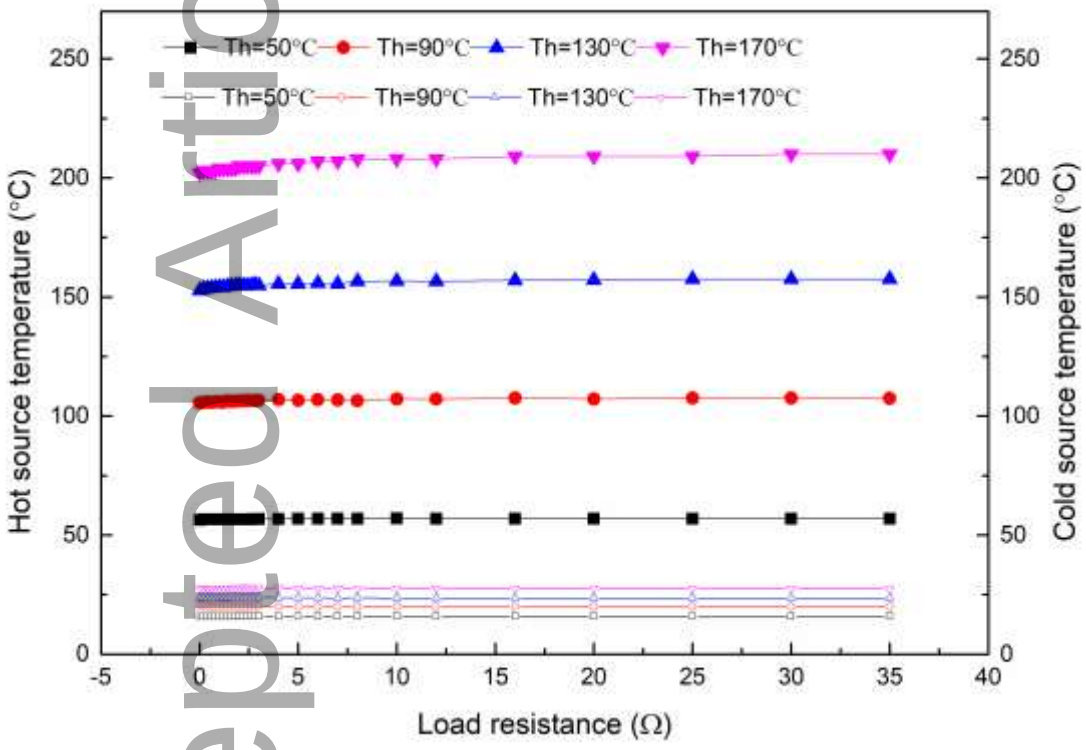

Figure 9 Source temperature variations at different hot side temperature of TEG

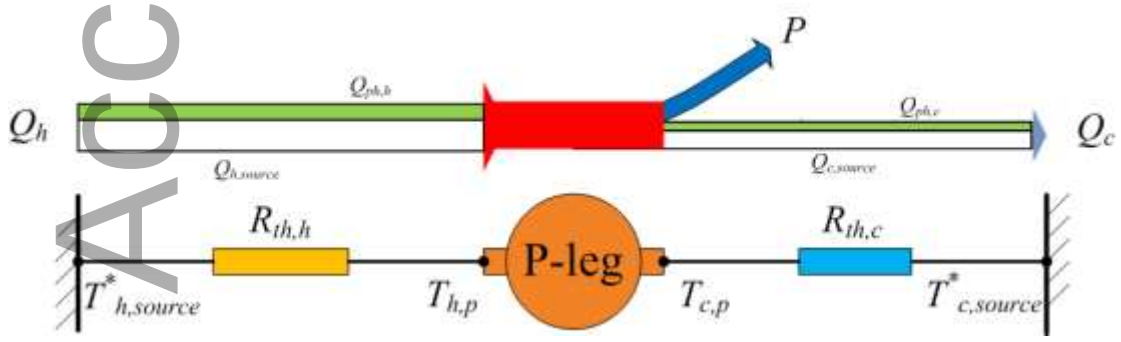

Figure 10 Thermal resistance and energy flow schematic diagram of P-type semiconductor

Figure 11 shows the percentage of the total temperature loss to the temperature difference at different hot side temperature. It can be seen that the total temperature loss gradually decreases to the zero with the increase of the load resistance. This is due to the reduction of the Peltier heat which

relies on the current. What's more, the percentage of the total temperature loss to the temperature difference increases with the increase of the hot side temperature at a certain load resistance, and the maximum percentage is 21.7% when the hot side temperature $T_{\square}$ is equal to the $170\square$ and the load resistance is close to 0Ω.

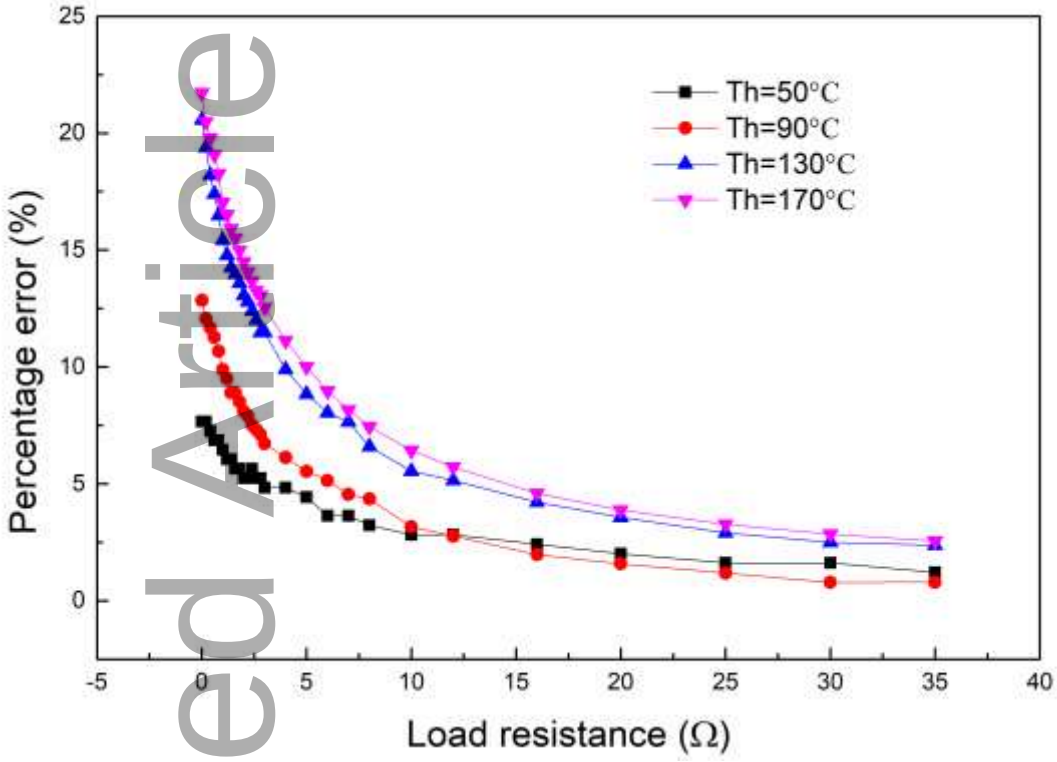

Figure 11 The percentage of total temperature loss to the temperature difference at different hot side temperature

4.4 Influence of Peltier effect on the input heat flow

The input heat flow $Q_{\square}$, conductive heat $Q_{c\square}$ and Peltier heat $Q_{p\square}$ with effective temperature difference at different hot side temperature are depicted in **Figure 12**. All of them almost have the linear relationship with effective temperature difference. Among the rest, the conductive heat increases linearly with the increase of the effective temperature difference, while the Peltier heat and the input heat flow decrease linearly with the increase of the effective temperature difference. In other words, although heat conduction determines the amount of total heat flow, Peltier effect governs the change trend of the total heat flow, then affects the change trend of the hot side temperature. And the same is true for heat transfer at the cold side, so that won't be covered again here.

Figure 13 shows the ratio of the Peltier heat $Q_{p\square}$ to the input heat flow $Q_{\square}$. It is found that the ratios at different hot side temperatures decrease with the increase of the load resistance. And the maximum ratio is up to 34.7%. The ratio also increases with the increase of the hot side temperature,

but the difference between temperatures is small. The variation of this ratio is similar to that of the percentage of total temperature loss to the temperature difference at different hot side temperature in **Figure 11**, that further explained the influence of Peltier effect on the temperature loss.

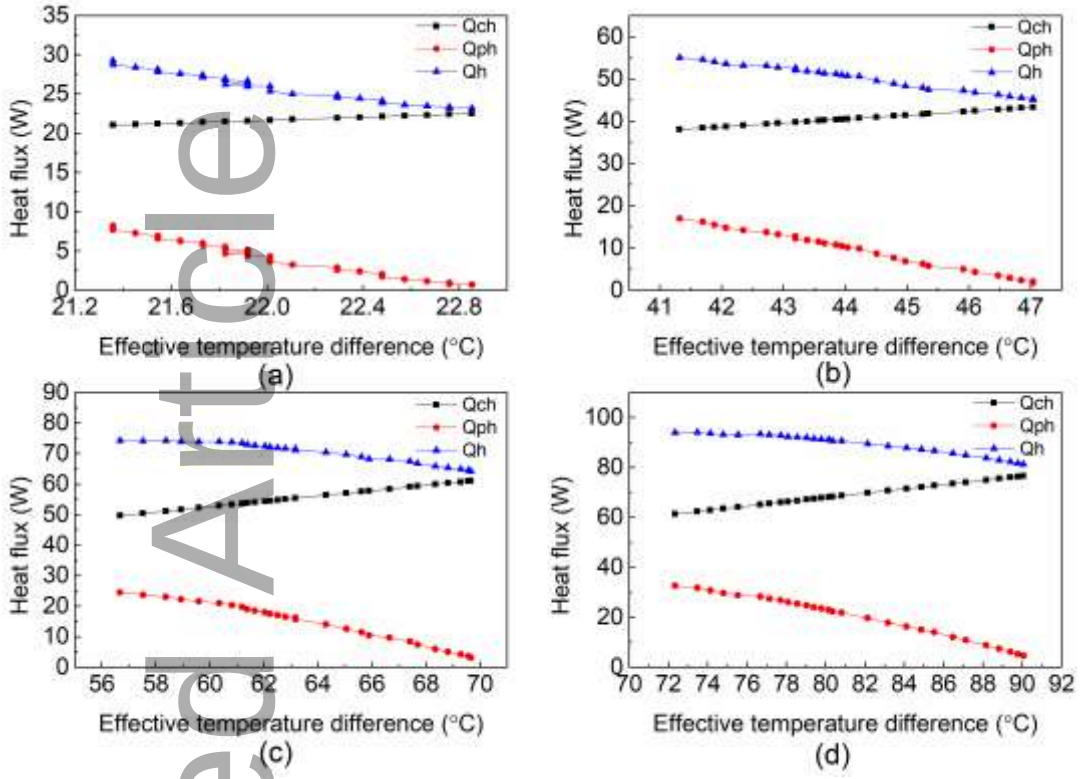

Figure 12 Heat flux variation at different hot side temperature （a）Th = 50□ (b) Th = 90□ (c) Th = 130□ (d) Th = 170□

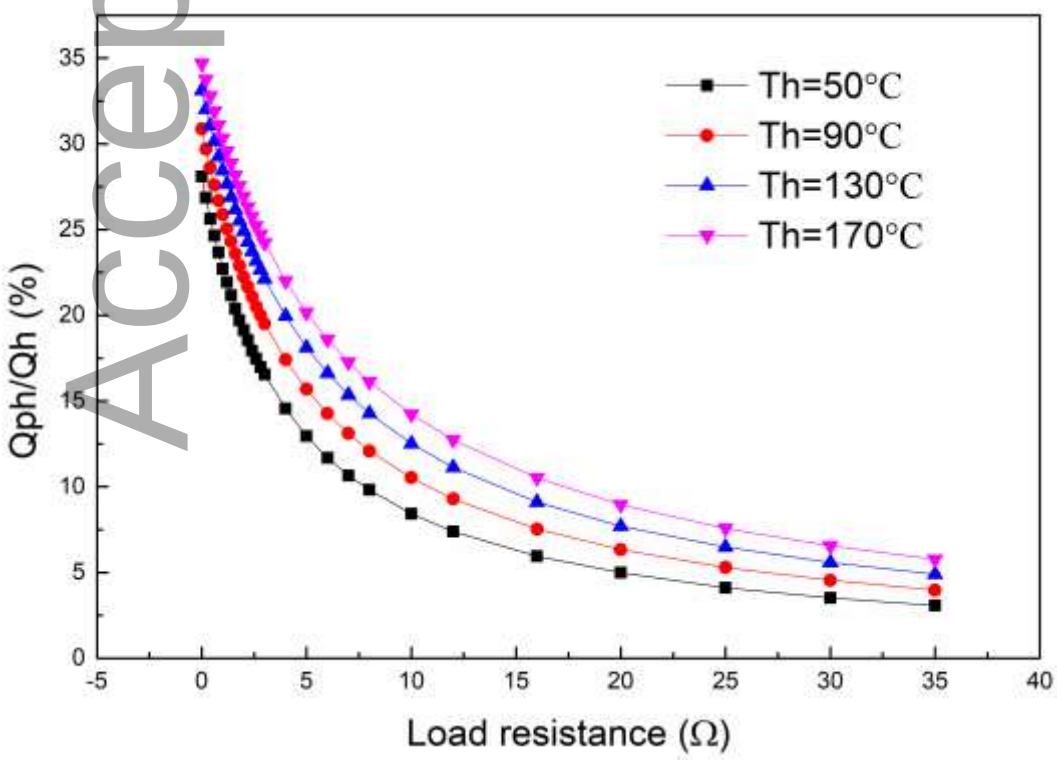

Figure 13 The ratio of the Peltier heat to the input heat flow at different hot side hot side temperature

4.5 Influence of Peltier effect on the loss of output power, energy efficiency and exergy efficiency

Figure 14 makes a comparison about output power with/without considering temperature loss at different hot side temperature and load resistance. The dash lines represent the calculated output power without considering temperature loss (i.e., the temperature conditions using output power calculations are at open-circuit state and the Peltier effect is ignored). It is clear that the output power considering the temperature loss is less than that of no temperature loss. That is due to the reduction of effective temperature difference caused by Peltier effect, which means the reduction of output voltage and current at the same time. What's more, the loss of output power increases with the increase of the hot side temperature and the maximum of the is up to 0.485W, taking up 34% of the maximum power, when hot side temperature is 170□. It can be explained that the Peltier heat is larger at hot side temperature. Finally, the loss of power loss rises at first and then declines with the increase of the load resistance. For this, if only the Peltier effect is considered, the maximum output power loss should appear in the near 0Ω, but it is not the case. The maximum output power loss is around the maximum power point. That is to say, the Seebeck effect dominates from the 0Ω to the load that the maximum power loss occurs and the Peltier effect is weakend partly in this range.

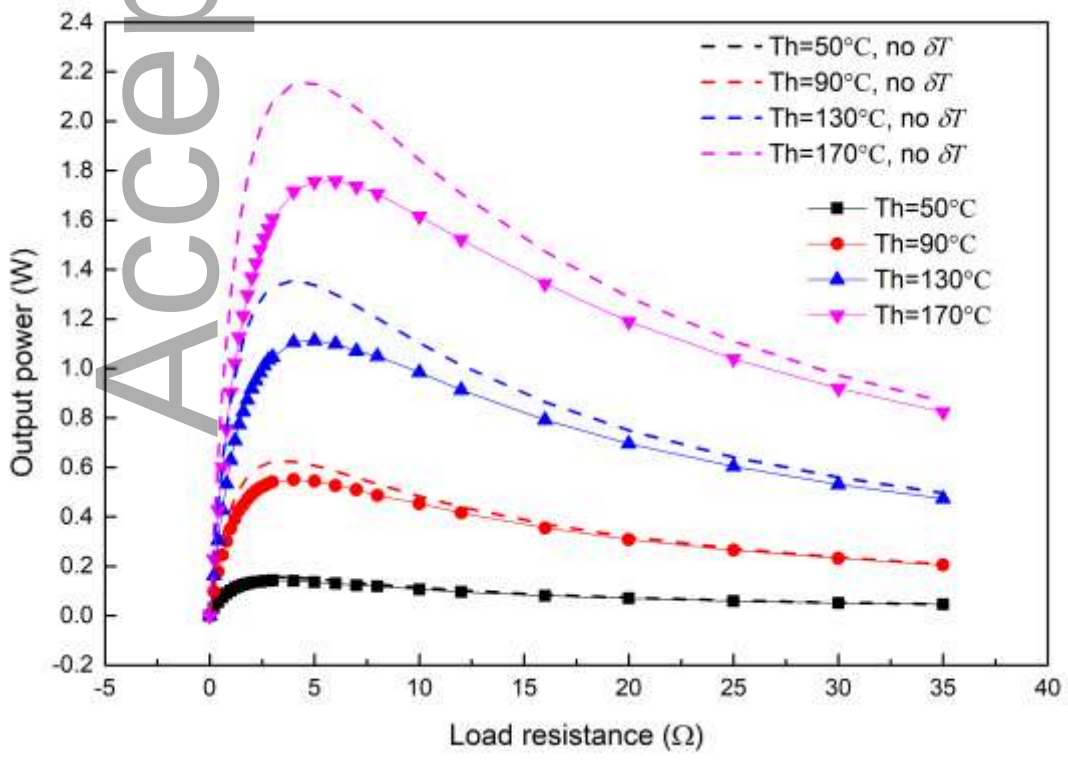

Figure 14 The variation of the output power with the load resistance

Figure 15 illustrates the variation of the power loss with the product of the effective temperature difference and total temperature loss $\Delta T \cdot \delta T$ at some representative loads, it is founded that the power loss almost has the linear relation with the $\Delta T \cdot \delta T$ at each load resistance. Through simple theoretical calculations, the power loss could be calculated as **Equation 24**:

$$\delta P = \frac{\alpha_{pn}^2 (2\Delta T \cdot \delta T + \delta T^2)}{R_{teg} + R_L} \quad (24)$$

In **Equation 24**, the δT^2 can be neglected because its amplitude is smaller than that of the $\Delta T \cdot \delta T$. Another fact that affects linearity is the temperature dependence of the internal resistance, but its influence is small. In addition, from **Figure 15**, it can be also seen that the power loss increases with the increase of the load resistance first and then decreases. The power loss at the 2.6Ω is nearly five times that at the 0.2Ω, when the hot side temperature is 170°.

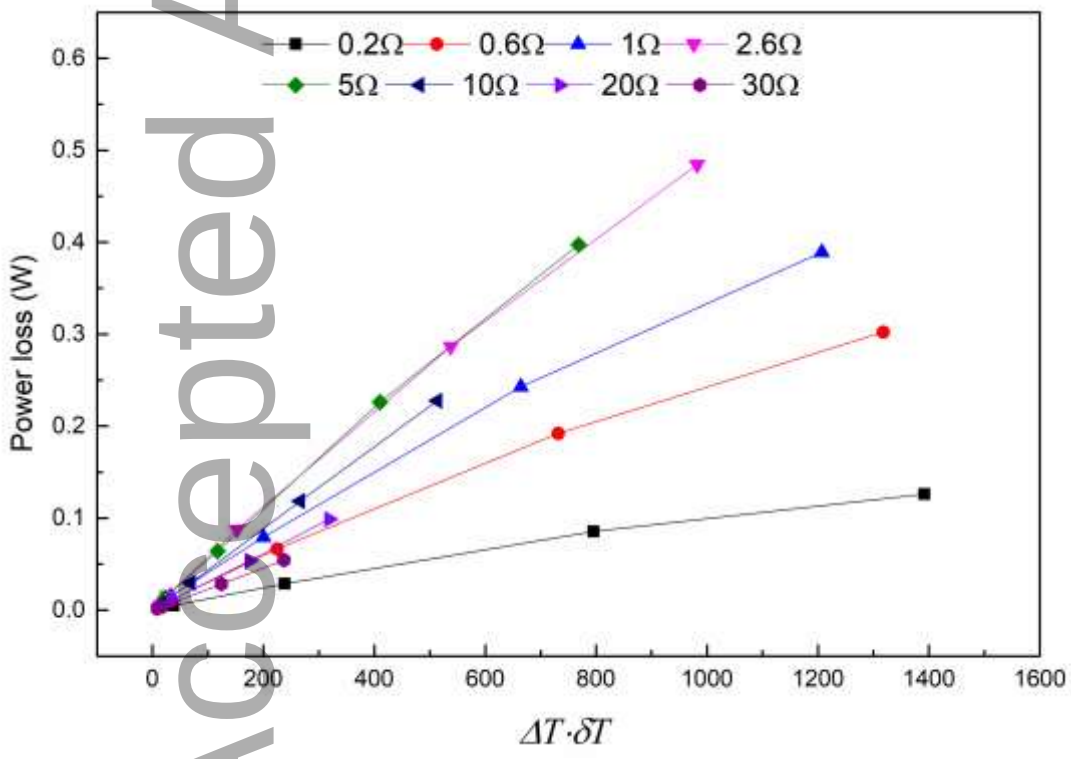

Figure 15 The variation of the power loss with $\Delta T \cdot \delta T$ at different load resistance

Figure 16 and **Figure 17** compare the variation of energy efficiency and exergy efficiency with/without temperature loss at different hot side temperatures respectively. For energy efficiency, its loss rises with the hot side temperature goes up. And its loss increases first and then decreases with the increase of the load resistance at each hot side temperature. In terms of exergy efficiency, the variation of its loss is similar to that of the energy efficiency. However, the maximum exergy efficiency loss is larger that of the energy efficiency.

When the exergy efficiency is higher than 50% of maximum exergy efficiency, the range of load resistance is effective[23]. **Figure 17** also depicts the effective load resistance ranges at different hot side temperatures. The effective load resistance range increases with the increase of the hot side temperature. There is no significant increase for the loss of exergy efficiency within the range of additional loads (i.e about 22Ω to 34Ω) from 50□ to 170□. In other words, increasing hot side temperature is desirable for more load resistance range.

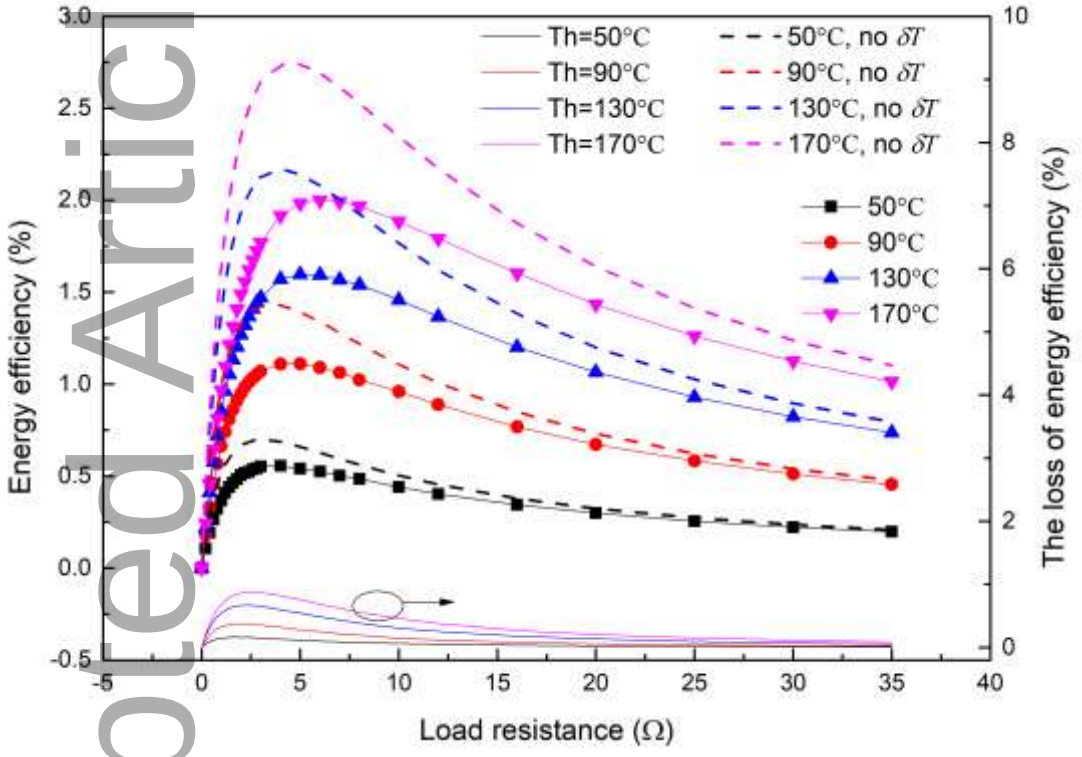

Figure 16 The variation of the energy efficiency and its loss with the load resistance

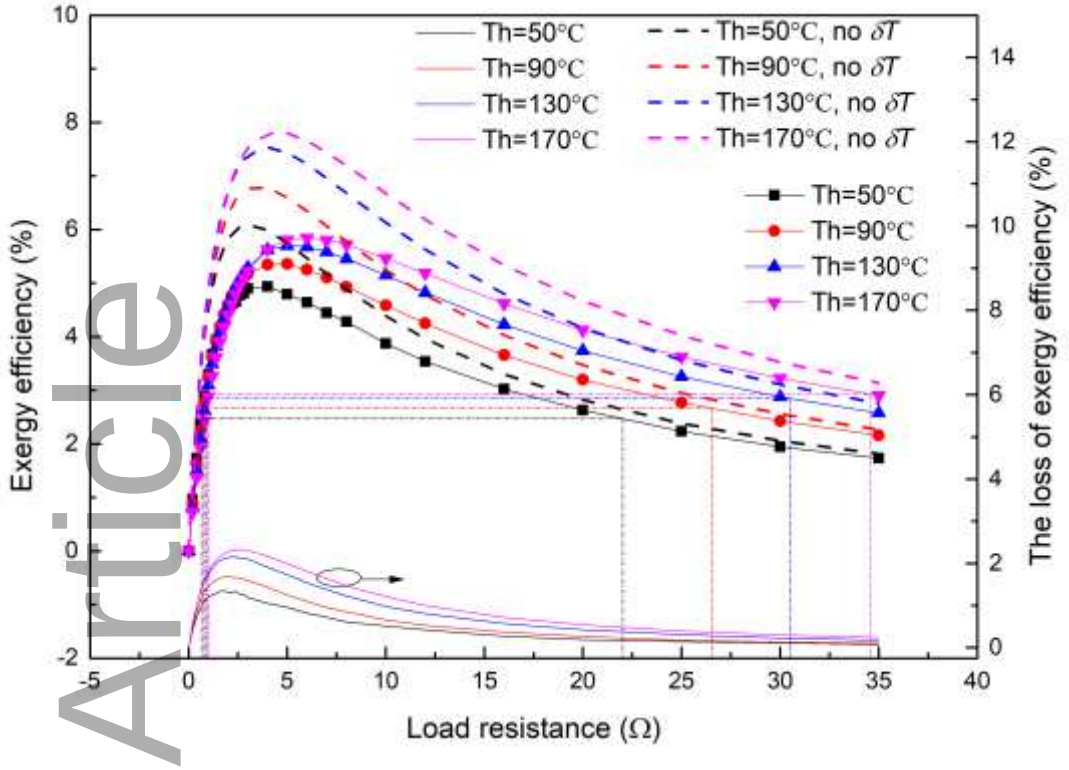

Figure 17 The variation of the exergy efficiency and its loss with the load resistance

5. Conclusion

To study the different impact of the Peltier effect on the temperature loss at two junctions of TEG and corresponding thermoelectric performance loss, an experimental setup and analytical model were adopted. The temperature loss at two sides, the loss of power, energy efficiency and exergy efficiency were chosen to evaluate the role of Peltier effect. In the experiment, the temperature at two side surfaces of TEG at different load resistance was obtained and was regarded as the boundary conditions of model. And the model was verified by experiment using open-circuit voltage. The following conclusions are obtained:

(1) At certain hot side temperature, the open-circuit voltage rises significantly first and then increases slightly to a constant when the cooling mode changes. And the open-circuit voltage increases with the increase of the hot side temperature.

(2) Peltier effect leads to temperature loss at both side of TEG and the loss decreases with the increase of the load resistance. And the percentage of the total temperature loss to the temperature difference also decreases gradually when the load resistance rises. Further, the hot junction temperature loss is larger than that of cold junction due to the difference of Peltier heat at two junctions. Reducing the thermal resistance at the hot side is more effective for larger temperature difference.

(3) The Peltier heat and the input heat flow decrease linearly with the increase of the effective temperature difference, so Peltier effect determines the variation trend of the total input heat flow. The ratios of the Peltier heat to the input heat flow at different hot side temperatures decrease with the increase of the load resistance.

(4) Peltier effect also brings about the loss of power, energy efficiency and exergy efficiency. All losses increase with the hot side temperature. They increase at first and then decrease with the load resistance meanwhile. However, the maximum loss does not occur where the Peltier effect is most obvious. The power loss has linear relation with the $\Delta T \cdot \delta T$. In addition, the effective load resistance range increases with the hot side temperature.

Acknowledgements

This work is financially supported by the National Natural Science Foundation of China (51776090). The authors gratelfully acknowledge financial support from China Scholarship Council.

Nomenclature

symbol			
A	Area (m^2)	h	Hot side of TEG
Ex	Exergy (W)	h,n	Hot side of N leg
H	Height (m)	h,p	Hot side of P leg
P_{out}	Output power (W)	hpn	The average at hot side of PN junction
Q_c	Output heat flow (W)	hpn,oc	The average at hot side of PN junction at open-circuit
Q_{ch}	Conductive heat (W)	$h,source$	Hot source
Q_h	Input heat flow (W)	in	Input
Q_{ph}	Peltier heat （W）	L	Load resistance
R	Electrical resistance (Ω)	m	average
R_{th}	Thermal Resistance (W^{-1})	n	N leg
T	Temperature (K / □)	o	Ambient environment
T^*	Ideal temperature (K / □)	oc	Open-circuit
U	Voltage (V)	out	Output
ΔT	Temperature difference (K / □)	p	P leg
δT	Temperature loss (K / □)	teg	Thermoelectric generator
δP	Power loss (W)		
		Abbreviations	
Subscripts		*TE*	Thermoelectric
c	Cold side of TEG	*TEG*	Thermoelectric generator
cm	Ceramic		
cp	Copper strips	Greek symbols	
c,n	Cold side of N leg	α	Seebeck coefficient (V/K)
c,p	Cold side of P leg	ε	Exergy efficiency
cpn	The average at cold side of PN junction	η	Energy efficiency
cpn,oc	The average at cold side of PN junction at open-circuit	λ	Thermal conductivity ($W \cdot m^{-1} \cdot K^{-1}$)
$c,source$	Cold source	ρ	Electrical resistance coefficient ($\Omega \cdot m$)

References

[1] A. Eldesoukey, H. Hassan, Energy Conversion and Management **2019**, *180*,231-239.

[2] H. He, W. Liu, Y. Wu, M. Rong, P. Zhao, X. Tang, Energy Conversion and Management **2019**, *180*,584-597.

[3] E. Kanimba, Z. Tian, Applied Thermal Engineering **2019**, *152*,858-864.

[4] A.S. Rattner, T.J. Meehan, Applied Thermal Engineering **2019**, *146*,795-804.

[5] H. Khalil, H. Hassan, Journal of Power Sources **2019**, *418*,98-111.

[6] H. Khalil, H. Hassan, Journal of Power Sources **2019**, *443*.

[7] A. Montecucco, J. Siviter, A.R. Knox, Applied Energy **2017**, *185*,1336-1342.

[8] Y. Sargolzaeiaval, V. Padmanabhan Ramesh, T.V. Neumann, V. Misra, D. Vashaee, M.D. Dickey, M.C. Öztürk, Applied Energy **2020**, *262*.

[9] S. Lan, A. Smith, R. Stobart, R. Chen, Applied Energy **2019**, *242*,273-284.

[10] X. Ma, G. Shu, H. Tian, W. Xu, T. Chen, Applied Energy **2019**, *248*,614-625.

[11] A. Marvão, P.J. Coelho, H.C. Rodrigues, Energy Conversion and Management **2019**, *179*,178-191.

[12] Y. Zhao, S. Wang, M. Ge, Z. Liang, Y. Liang, Y. Li, Applied Energy **2019**, *239*,425-433.

[13] D. Champier, Energy Conversion and Management **2017**, *140*,167-181.

[14] W.-H. Chen, Y.-X. Lin, X.-D. Wang, Y.-L. Lin, Applied Energy **2019**, *241*,11-24.

[15] A. Ferrario, S. Boldrini, A. Miozzo, M. Fabrizio, Applied Thermal Engineering **2019**, *150*,620-627.

[16] G. Li, Y. Zheng, J. Hu, W. Guo, Energy **2019**, *185*,437-448.

[17] S. Wang, T. Xie, H. Xie, Applied Thermal Engineering **2018**, *130*,847-853.

[18] K. Karthick, S. Suresh, H. Singh, G.C. Joy, R. Dhanuskodi, Renewable Energy **2019**, *134*,25-43.

[19] A.B. Zhang, B.L. Wang, D.D. Pang, L.W. He, J. Lou, J. Wang, J.K. Du, Energy **2018**, *147*,612-620.

[20] M. Liao, Z. He, C. Jiang, X.a. Fan, Y. Li, F. Qi, Applied Thermal Engineering **2018**, *133*,493-500.

[21] J. Wang, P. Cao, X. Li, X. Song, C. Zhao, L. Zhu, Energy Conversion and Management **2019**, *200*.

[22] D.R. Karana, R.R. Sahoo, Energy **2019**, *179*,90-99.

[23] H. Nami, A. Nemati, M. Yari, F. Ranjbar, Applied Thermal Engineering **2017**, *124*,756-766.

[24] S. Manikandan, S.C. Kaushik, Solar Energy **2016**, *135*,569-577.

[25] S.C. Kaushik, S. Manikandan, Energy Conversion and Management **2015**, *103*,200-207.

[26] S. Manikandan, S.C. Kaushik, Energy **2016**, *100*,227-237.

[27] Y. Cai, W.-W. Wang, C.-W. Liu, W.-T. Ding, D. Liu, F.-Y. Zhao, Renewable Energy **2020**, *147*,1565-1583.

[28] S. Asaadi, S. Khalilarya, S. Jafarmadar, Applied Thermal Engineering **2019**, *156*,371-381.

[29] S. Vostrikov, A. Somov, P. Gotovtsev, Applied Energy **2019**, *255*.

[30] P. Wang, B.L. Wang, J.E. Li, International Journal of Heat and Mass Transfer **2019**, *143*.

Influences of Peltier effect on the temperature loss at both sides of thermoelectric generator are studied. The temperature loss at the cold side of thermoelectric generator is less than that of the hot side. The maximum loss of power, energy and exergy efficiency occurs at a particular load range, where power, energy and exergy efficiency reach the maximum respectively.

Xingjun Li, Jun Wang, Qingtian Meng, Dan Yu

Theoretical and experimental investigation about the influence of Peltier effect on the temperature loss and performance loss of thermoelectric generator